

First-order and tricritical wetting transitions in the two-dimensional Ising model caused by interfacial pinning at a defect line

Marta L. Trobo

Instituto de Física de Líquidos y Sistemas Biológicos (IFLYSIB), CCT-CONICET La Plata, UNLP. Calle 59 Nro. 789, (1900) La Plata, Argentina and Facultad de Ingeniería, Universidad Nacional de La Plata, Argentina

Ezequiel V. Albano

Instituto de Física de Líquidos y Sistemas Biológicos (IFLYSIB), CCT-CONICET La Plata, UNLP. Calle 59 Nro. 789, (1900) La Plata, Argentina and Facultad de Ciencias Exactas, Universidad Nacional de La Plata, Argentina

Kurt Binder

Institut für Physik, Johannes Gutenberg-Universität Mainz, Staudinger Weg 7, D-55099 Mainz, Germany

(Received 16 May 2014; published 18 August 2014)

We present a study of the critical behavior of the Blume-Capel model with three spin states ($S = \pm 1, 0$) confined between parallel walls separated by a distance L where competitive surface magnetic fields act. By properly choosing the crystal field (D), which regulates the density of nonmagnetic species ($S = 0$), such that those impurities are excluded from the bulk (where $D = -\infty$) except in the middle of the sample [where $D_M(L/2) \neq -\infty$], we are able to control the presence of a defect line in the middle of the sample and study its influence on the interface between domains of different spin orientations. So essentially we study an Ising model with a defect line but, unlike previous work where defect lines in Ising models were defined via weakened bonds, in the present case the defect line is due to mobile vacancies and hence involves additional entropy. In this way, by drawing phase diagrams, i.e., plots of the wetting critical temperature (T_w) versus the magnitude of the crystal field at the middle of the sample (D_M), we observe curves of (first-) second-order wetting transitions for (small) high values of D_M . These lines meet in tricritical wetting points, i.e., (T_w^{tc}, D_M^{tc}) , which also depend on the magnitude of the surface magnetic fields. It is found that second-order wetting transitions satisfy the scaling theory for short-range interactions, while first-order ones do not exhibit hysteresis, provided that small samples are used, since fluctuations wash out hysteretic effects. Since hysteresis is observed in large samples, we performed extensive thermodynamic integrations in order to accurately locate the first-order transition points, and a rather good agreement is found by comparing such results with those obtained just by observing the jump of the order parameter in small samples.

DOI: [10.1103/PhysRevE.90.022406](https://doi.org/10.1103/PhysRevE.90.022406)

PACS number(s): 68.08.Bc, 64.60.De, 05.70.Fh

I. INTRODUCTION

The study and characterization of surfaces and interfaces is a relevant topic in many fields of physics, chemistry, material science, etc. [1,2], and has undergone long-standing study. In fact, considerable experimental and theoretical attention has been addressed to understanding common features of surfaces and interfaces at equilibrium [3–8] and far from it [9,10]. This broad interest is motivated not only by numerous and interesting technological applications but also by the existence of many challenges at the basic level. Within this broad context, the influence of the presence of an additional phase at the interface between two phases has also been the subject of experimental and theoretical studies. In particular, the enhancement of the density of the additional phase at the interface is known as “interfacial adsorption.” An experimental realization of this physical situation is provided by a two-component fluid system in equilibrium with its vapor phase [11]. From the point of view of statistical physics, which is the approach that will be developed in this paper, interfacial adsorption can be studied with the aid of three-state models, such as Potts and Blume-Capel (BC) models [12,13]. Focusing our attention on the BC model with three spin states ($S = \pm 1, 0$ where 0 corresponds to the vacancies or nonmagnetic impurities) a straightforward way to observe

interfacial adsorption is by confining the sample between two walls where competitive surface magnetic fields act. In this way, an interface between domains of different signs of the magnetization runs parallel to the confining walls, and vacancies adsorb preferentially along such an interface leading to interfacial adsorption, as reported by Selke [14]. It is also known that, depending on the temperature and the magnitude of the competitive surface fields, the interface between domains undergoes localization-delocalization “transitions.” Those “effective” transitions are the precursors of the wetting transitions observed when the thermodynamic limit is properly taken. Interfacial adsorption has been observed by studying the localization-delocalization transition of the interface between domains of different magnetization in the BC model [15]. Furthermore, very recently, Fytas and Selke [16] have reported an extensive numerical study of wetting and interfacial adsorption in the BC model. In order to study wetting behavior in $d = 2$ dimensions, Fytas and Selke assumed that spins are fixed at the boundaries with two different states, “+1” and “−1.” Furthermore, reduced couplings (by a factor α) are taken at one boundary. The adsorption of “0” spins at the interface between “−1” and “+1” rich regions is mainly characterized by measuring the interfacial adsorption W_0 , which accounts for the surplus of “0” spins caused by the presence of the

interface. It is reported that due to the strong meandering of the interface, W_0 grows rapidly when approaching the wetting temperature. The existence of a singularity in the temperature derivative of W_0 at the wetting transition is conjectured. Furthermore, it is worth mentioning that the results of Fytas and Selke for the wetting transition of the BC model confined between walls are in agreement with previous results [15] and are found to obey the recently proposed anisotropic scaling behavior for wetting transitions with short-range surface fields [15,17].

In a related context, great interest has also been attracted by the study of interfacial pinning induced by impurities. In fact, experimental and theoretical evidence [18,19] has confirmed that a magnetic interface can be pinned by nonmagnetic impurities distributed uniformly. In particular, if the impurities are grouped forming aligned triangles, it is found that pinning is more efficient when the interface approaches the triangle by its basis as compared to the case of approaching it by one vertex. This preferential pinning causes an interesting interfacial crossed-ratchets effect. Also, the influence of nonmagnetic fixed impurities placed at the center of an Ising ferromagnet confined between walls has been studied [20]. It is found that for a low density of impurities the wetting transition remains continuous (second order), while abrupt first-order transitions are observed when such a density increases. In view of the reported change in the nature of the wetting transition caused by the presence of impurities in the case of the Ising ferromagnet, it is surprising that interfacial adsorption in the BC model does not affect the second-order nature of the wetting transition [15,16].

Within this broad context, the aim of the present paper is to contribute to understanding the role played by nonmagnetic impurities or vacancies forming a line of defects in the wetting transition that occurs in the Ising ferromagnet confined between walls where competitive surface magnetic fields act. For this purpose we studied the confined BC model by means of extensive Monte Carlo simulations. In particular, we assume that the crystal field (D) that regulates the concentration of nonmagnetic impurities is $D = -\infty$ in the bulk, so impurities are expelled and the BC model is mapped into the standard Ising model. However, by taking $D > -\infty$ at the center of the stripped geometry, we are able to properly regulate the density of nonmagnetic impurities in the central region where the interface starts to be fully delocalized at the wetting transition (the details of the BC Hamiltonian used are given below). By using the approach discussed above, we are able to elucidate the role played by a line of nonmagnetic impurities in the onset of first-order and tricritical wetting transitions [4,6,21] in the $d = 2$ dimensional BC model.

Here we would like to stress the relevance of the present manuscript for the understanding of tricritical wetting in $d = 2$ dimensions, within the broad context of basic studies in the field of statistical mechanics. In fact, it is worth mentioning that the mean-field theory of wetting transitions with short-range surface forces [4,6,7,21–23] shows that both first-order and second-order wetting transitions may occur. However, in $d = 2$ dimensions, Ginzburg-Landau-type [22,23] theories are very unreliable [24] since statistical fluctuations are neglected. Also, the tricritical wetting behavior in $d = 2$ beyond the mean field was only occasionally considered [25]. On the other hand,

the numerical studies of Cotes and Albano [20] have suggested qualitatively the possible observation of tricritical wetting when a certain fraction (F_v) of fixed vacancies or nonmagnetic impurities are equidistantly placed along a line at the center of a confined Ising magnet. In fact, first-order wetting transitions are located qualitatively by observing negative peaks of the cumulant, as well as abrupt drops of the magnetization of the system. In this way the accuracy in the location of the transitions is largely affected by hysteretic effects. Furthermore, second-order wetting transitions are also located with large uncertainties due to the lack of a suitable scaling theory, which was developed only later [15,17]. In contrast, in the present work we provide unambiguous evidence of the existence of tricritical wetting in $d = 2$ dimensions since critical wetting points are accurately determined by means of the intersection method that follows from the proper scaling theory [15,17], while first-order wetting transitions are carefully located by means of the thermodynamic integration method [26,27].

Furthermore, from the basic point of view, wetting behavior with fixed impurities of constant density [20], differs markedly from the case of mobile impurities with temperature-dependent density reported here. In fact, as discussed in detail in Sec. IV, the location of the wetting transition depends on the wall excess free-energy difference $f_s^{(+)} - f_s^{(-)}$ between semi-infinite systems with positive (+) and negative (−) spontaneous magnetization, both exposed to a positive boundary field, and the interfacial tension between bulk coexisting phases [$f_{\text{int}}(T)$], according to Young's criterion [3,4], namely $f_s^{(+)} - f_s^{(-)} = f_{\text{int}}(T)$. While the presence of vacancies at the center of the sample is expected to cause an almost negligible effect on the wall excess energy, the nature of these vacancies, i.e., mobile versus fixed, dramatically affects the interfacial tension. For a fixed line of vacancies, as considered in Ref. [20], ground-state considerations yield $f_{\text{int}}^{\text{FV}}(T = 0)/J = 2(1 - F_v)$, exactly for $F_v \leq 1/2$, where J is the coupling constant. In this way, the Onsager result [28] $f_{\text{int}}^{\text{Ons}}(T = 0)/J = 2$ is recovered in the absence of vacancies. On the other hand, for the case of mobile vacancies treated here, one also has that $f_{\text{int}}^{\text{MV}}(T = 0)/J = 2$, since the density of vacancies vanish for $T \rightarrow 0$ and the values of the crystal field considered. So, based on free-energy considerations and the small difference between $f_{\text{int}}^{\text{FV}}(0 < T < T_{\text{cb}})$ and $f_{\text{int}}^{\text{Ons}}(0 < T < T_{\text{cb}})$, where T_{cb} is the bulk critical temperature of the system, the onset of complete wetting in the case of mobile vacancies confined to the middle of the sample is quite unexpected.

Within this latter context, it is also worth noting the difference between standard interfacial adsorption that does not change the order of the wetting transition [15,16] and the interfacial pinning by mobile vacancies studied here. In both cases vacancies are mobile: When they can follow the displacements of the interface the wetting transition remains second order, but, in contrast, when they are mobile but constrained to a line of defects they can pin the interface (provided that a certain threshold density is achieved). In this way our simple model gives insight into the role played by constrained mobile impurities in the stabilization of interfacial fluctuations. Experimentally, this might correspond to the pinning of domain walls by dislocations, for instance. On

the other hand, a line of fixed and equidistant vacancies can be thought of as a quenched perturbation, while, in contrast, the case studied here the perturbation is more likely related to the treatment of annealed disorder and, consequently, merits further and independent consideration. Summing up, we conclude that both interfacial adsorption [15,16] and the system studied in Ref. [20] address completely different physical situations, from many points of view, from that treated here.

Furthermore, statistical mechanic studies of the effect of vacancies confined along a line on the wetting behavior is relevant not only for the understanding of the role played for a line of defects but also for the case where weakened coupling constants along a line is considered (recall that vacancies effectively screen out the interactions between spins). In fact, the effect caused by a line of weakened bonds in the wetting behavior of the two-dimensional Ising ferromagnet [29,30] and in related solid-on-solid (SOS) models [31–34] has been considered by using different methods, such as analytical exact solutions [29,30], transfer matrix calculations [31–35], random walk arguments [36], renormalization group calculations [37], numerical simulations [35], and so on.

Also, various geometries have been used: by taking a line of weakened bonds along two slabs each of them with the same coupling constant one has a critical wetting transition when the line is close to the walls (i.e., the well-known result worked out exactly by Abraham [29]), but no wetting transition is found if the line is far away from the wall since a line of weakened bonds in the interior of a planar Ising ferromagnetic lattice always binds a domain wall [30]. That exact result has also been recovered by using random walk arguments [36] and by considering SOS models [33,34]. However, transfer matrix calculations in a SOS model show that a critical wetting transition occurs whenever the couplings on the two sides of the defect differ [34]. So the occurrence of tricritical wetting reported here reflects the subtle effect due to mobile vacancies that involves additional entropy as compared to the previously considered cases of weakened bonds.

Finally, we would like to mention that the case of mobile vacancies could be relevant for the study of wetting upon adsorption on layered materials, e.g., when two bulky layers (of a single or different compound) are separated by a very thin layer of an additional species, as used in many micro- and nanodevices. Another realization would be a binary surfactant mixture at the air-water interface undergoing phase separation: A defect line with mobile particles then could be created by colloidal particles bound also to the interface but trapped in a cylindrical potential well at the interface, created by suitable laser fields. This system would be a direct (qualitative) realization of the situation envisaged in our simple model.

The manuscript is organized as follows: in Sec. II we describe the main features of the BC Hamiltonian used together with a brief discussion of the simulation method. Section III is devoted to the presentation and discussion of our results within the framework of the finite-size scaling approach for wetting transitions with short-range surface fields [17]. In Sec. IV we describe and apply the thermodynamic integration method for the location of first-order wetting transitions, and, finally, our conclusions are stated in Sec. V.

II. THE BLUME-CAPEL MODEL IN A CONFINED GEOMETRY AND DETAILS OF THE SIMULATION METHOD

A. The model

We consider the Hamiltonian of the three-state Blume-Capel model [12,13] where each lattice site of coordinates (i, j) carries a spin S_{ij} that can take on the values $S_{ij} = \pm 1, 0$. We take a square lattice in an $L \times M$ geometry with $1 \leq i \leq L$, and $1 \leq j \leq M$, where periodic boundary conditions act in the j direction (where the lattice is M rows long), while free boundary conditions are used in the i direction, where we apply boundary fields H_1, H_L acting on the first and last rows, respectively. Thus, the BC Hamiltonian is given by

$$\mathcal{H} = -J \sum_{\langle ij, i'j' \rangle} S_{ij} S_{i'j'} + \sum_i D(i) \sum_j S_{ij}^2 - H_1 \sum_{i \in \text{row } 1, j} S_{ij} - H_L \sum_{i \in \text{row } L, j} S_{ij}, \quad (1)$$

where $J > 0$ is the coupling constant between spins placed at nearest-neighbor sites, which we take as homogeneous throughout the system, and the symbol $\langle ij, i'j' \rangle$ indicates that the summation is restricted to nearest-neighbor spins only. $D(i)$ denotes the strength of the crystal field, measured in units of J , which regulates the concentration of nonmagnetic impurities. Specifically, we assume (note we always take L to be even)

$$D(i) = \begin{cases} D_M & \text{for } i = L/2, L/2 + 1 \\ -\infty, & \text{otherwise.} \end{cases} \quad (2)$$

For the study of wetting transitions or, more rigorously, localization-delocalization “effective” transitions occurring in finite samples, it is convenient to adopt the antisymmetric situation $H_1 = -H_L < 0$ and then consider the thermodynamic limit ($L \rightarrow \infty, M \rightarrow \infty$) in order to observe a true wetting transition.

It is well known that, in the two-dimensional Blume-Capel model, in the absence of magnetic fields and with a constant crystal field D , which leads to a homogeneous distribution of nonmagnetic impurities, one has a nontrivial bulk phase diagram with a tricritical point [38]. For the square lattice, this tricritical point occurs at $D_t/J = 1.965$ and $k_B T_t/J = 0.609$ [38,39]. For $D > D_t$ the transition at $T_c(D)$ is of first order, while for $D < D_t$ the transition becomes of second order.

In our case, with an inhomogeneous density of nonmagnetic impurities, competitive surface fields, and for $D < D_t$, the system undergoes two types of phase transition: For temperatures $T_{cb}(D)$, phase transitions occur from the disordered “paramagnetic” phase to the ordered “ferromagnetic” phase, where we have used the terminology of the Ising model. In fact, for $D = -\infty$ the BC model maps into the Ising model since vacancies are excluded, and for the particular choice of the crystal field used here [see Eq. (2)] we expect that $T_{cb}(D) = T_{cb}$, with $\exp(2J/k_B T_{cb}) = \sqrt{2} + 1$, where $T_{cb} \simeq 2.27J/k_B$ is the bulk critical temperature of the $d = 2$ Ising model. However, a second type of phase transition (i.e., wetting transitions) occurs at lower temperatures $T_w(H_1) \leq T_{cb}(D)$ for small-enough absolute values $|H_1|$ of the surface field. Thus, below $T_w(H_1)$ the surface field stabilizes a macroscopically

thick layer of negative magnetization near the boundary where $H_1 < 0$ acts, separated by an interface from the bulk, where the magnetization is positive. At $T_w(H_1)$, a transition occurs where this interface gets delocalized. This localization-delocalization “transition” is the precursor of a true wetting transition occurring in the thermodynamic limit [15,17]. In the Ising model, which results from Eq. (1) as the limiting case $D_M \rightarrow -\infty$, this wetting transition is of second order throughout the regime $0 < |H_1| < J$.

B. Simulation method and numerical details

We performed Monte Carlo simulations by using the standard Metropolis algorithm, and we measured the time in units of Monte Carlo steps per spin (MCS), i.e., during each MCS all the $L \times M$ spins of the sample have the chance of reversing their orientations (flipping) at least once, on average. Typical runs are performed over 4×10^6 MCS, discarding the first 1×10^6 MCS to allow for equilibration.

According to the finite-size scaling theory for wetting transitions with short-range interactions [15,17], all simulations are performed for the choice $c = L^2/M = 9/8$ of the generalized aspect ratio, which allows for a set of integer solutions of L and M , i.e., values such as $(L, M) = (12, 128), (18, 288), (24, 512), (36, 1152)$, and $(48, 2048)$, which are commonly used in our calculations.

During the simulations, we evaluated the total average absolute magnetization of the film, $\langle |m| \rangle$, obtained from the magnetization m per lattice site,

$$m = \frac{1}{N} \sum_{k=1}^N S_k, \quad (3)$$

which involves the summation over the total number of spins ($N = L \times M$) in the sample, and $\langle \rangle$ indicates thermal averages over different configurations obtained after disregarding a suitable number of MCS in order to allow for equilibration. We also computed the square value of magnetization $\langle m^2 \rangle$, and the fourth-order cumulant, which is given by

$$U = 1 - \frac{\langle m^4 \rangle}{3\langle m^2 \rangle^2}. \quad (4)$$

Also, magnetization and impurity density profiles across the film $m(i)$ and $\zeta(i)$ with $1 \leq i \leq L$ are evaluated, respectively.

III. RESULTS AND DISCUSSION

In order to gain insight into the role of mobile and nonconserved impurities located along the center of the strip, we performed extensive Monte Carlo simulations scanning a broad interval of each relevant parameter, namely $-3 \leq D_M/J \leq 0$, $0.6 \leq H_1/J \leq 0.80$, and $0.4 \leq T/T_{cb} \leq 1.0$, where T_{cb} is the bulk critical temperature of the Ising model. The analysis of the data reveals two distinct scenarios: on the one hand, the occurrence of second-order wetting transitions for smaller values of D_M and, on the other hand, the observation of sharp first-order wetting transitions for large values of D_M . In fact, Fig. 1 shows plots of $\langle |m| \rangle$, $\langle m^2 \rangle$ and the cumulant U versus T/T_{cb} obtained for $D_M/J = -2$ and $H_1/J = 0.60$.

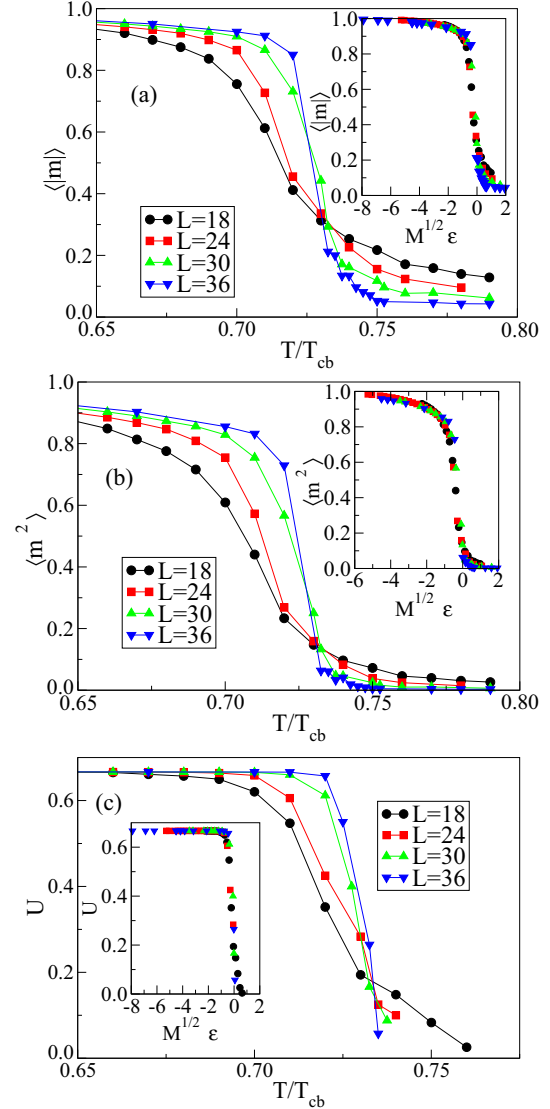


FIG. 1. (Color online) Plots of (a) the average absolute value of the magnetization ($\langle |m| \rangle$), (b) the average square magnetization ($\langle m^2 \rangle$), and (c) the cumulant (U) versus the temperature relative to the bulk critical point, obtained for samples of different sizes (as indicated). Data corresponding to $D_M/J = -2.0$ and $H_1/J = 0.60$. All sample sizes have the same generalized aspect ratio $c = L^2/M = 9/8$. The common intersection point at $T_w/T_{cb} = 0.735 \pm 0.015$ allows us to locate the critical wetting temperature [15]. The insets in these figures show the corresponding scaling plots of the observable already shown in the main panel [15]. Further details are given in the text.

The data corresponding to four different lattice sizes show smooth variations of the observables that are consistent with a second-order wetting transition.

It is well known that the critical properties of the transition are governed by two correlation lengths, in the directions parallel (ξ_{\parallel}) and perpendicular (ξ_{\perp}) to the interface between domains of different magnetization, which diverge at criticality according to

$$\xi_{\parallel} \sim \epsilon^{-\nu_{\parallel}}, \quad (5)$$

with $\epsilon = (T - T_w)$, and

$$\xi_{\perp} \sim \epsilon^{-\nu_{\perp}}, \quad (6)$$

respectively. Here T_w is the critical point of the wetting transition, while $\nu_{\parallel} = 2$ and $\nu_{\perp} = 1$ are the correlation length exponents in the parallel and perpendicular directions to the interface, respectively. Due to the anisotropic physical situation, the data must be analyzed by using anisotropic scaling, of course. Very recently, we have shown, using finite systems with antisymmetric short-range surface fields as in the present study, that wetting transitions can be rationalized in terms of a bulk transition, $\langle |m| \rangle$ being the proper order parameter [15]. But in this case the order parameter critical exponent is $\beta = 0$. In general, the scaling behavior of the order parameter and its moments are given by

$$\langle |m| \rangle = \xi_{\parallel}^{-\beta/\nu_{\parallel}} \tilde{m} \left(\frac{L^{\nu_{\parallel}/\nu_{\perp}}}{M}, \frac{M}{\xi_{\parallel}} \right) \quad (7)$$

and

$$\langle m^{2k} \rangle = \xi_{\parallel}^{-2k\beta/\nu_{\parallel}} \tilde{m}^{2k} \left(\frac{L^{\nu_{\parallel}/\nu_{\perp}}}{M}, \frac{M}{\xi_{\parallel}} \right), \quad (8)$$

respectively. Here \tilde{m} and \tilde{m}^{2k} are suitable scaling functions that do not need to be specified. Due to the fact that $\beta = 0$, one has that the prefactors of the scaling functions become constant in both Eqs. (7) and (8). Furthermore, plots of $\langle |m| \rangle$ and all its moments would exhibit a common intersection point at criticality, as already observed in Fig. 1. Of course, the above statement holds if the generalized aspect ratio $c = L^{\nu_{\parallel}/\nu_{\perp}}/M = L^2/M$ is kept constant, as follows from the first scaling argument in Eqs. (7) and (8). Since the prefactor of the cumulant is already independent of the lattice site, the intersection point in curves of U versus T/T_{cb} obtained for samples of different sizes also coincides with the previously discussed ones (see Fig. 1), namely the intersection points observed for $\langle |m| \rangle$ and $\langle m^2 \rangle$. In this way, the critical point of the corresponding wetting transition is given by $T_w/T_{cb} = 0.735 \pm 0.015$ for $D_M/J = -2$ and $H_1/J = 0.60$. We advanced one further step by testing the scaling behavior [15] given by Eqs. (7) and (8) [see the insets of Figs. 1(a)–1(c)] that is nicely verified by the quality of the observed data collapse.

On the other hand, when considering larger values of D_M , one observes abrupt first-order wetting transitions as, e.g., is shown in Fig. 2 for $D_M = -1$. In fact, plots of $\langle |m| \rangle$ versus T/T_{cb} obtained for $H_1/J = 0.8$ and relatively small lattices ($L \leq 30$, with $c = L^2/M = 9/8$) show an abrupt transition at the wetting temperature $T_w/T_{cb} = 0.511 \pm 0.005$ that is almost independent of the lattice size. Furthermore, we do not observe hysteretic effects for those sample sizes. However, a hysteresis loop is already observed for bigger samples [see the inset of Fig. 2(a) for $L = 48$]. So, presumably, fluctuations of spacial size of the order of the smaller lattice sizes prevent the occurrence of hysteresis, and, consequently, the latter is observed only in larger systems. Additional evidence supporting the existence of first-order behavior is provided by the cumulant [see Fig. 2(b)] that exhibits sharp negative peaks at the transition point [40].

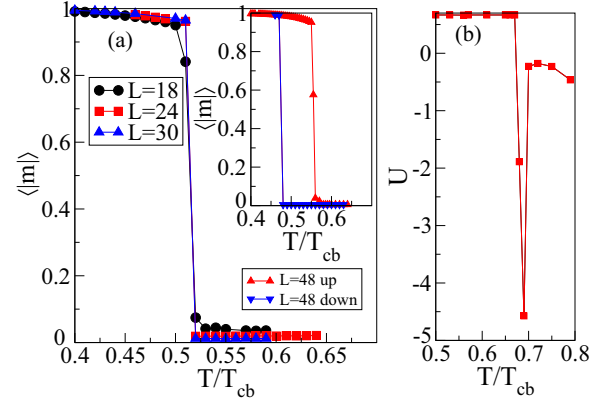


FIG. 2. (Color online) (a) Plots of the average absolute value of the magnetization ($\langle |m| \rangle$) versus T/T_{cb} obtained for samples of different sizes (as indicated). Data corresponding to $D_M/J = -1.0$, $H_1/J = 0.80$. The main panel shows the absence of hysteresis in small samples, while the inset shows that hysteretic effects become appreciable by using larger samples where the initial conditions are with all spins pointing up and down, respectively. (b) Plot of the cumulant (U) versus T/T_{cb} as obtained for samples of sizes $L = 36$, $M = 1152$, $D_M/J = -1.0$, $H_1/J = 0.60$. The sharp negative peak of U is a signature of a first-order wetting transition [40] as already evidenced in part (a). Further details are given in the text.

Figure 3 shows a comparison of the magnetization profiles measured along the direction perpendicular to the interface. Figure 3 also shows the impurity density profiles that exhibit a peak just at the center of the sample where $D_M > -\infty$ and, consequently, the presence of impurities becomes enhanced. The profiles shown in Fig. 3(a) were obtained at the

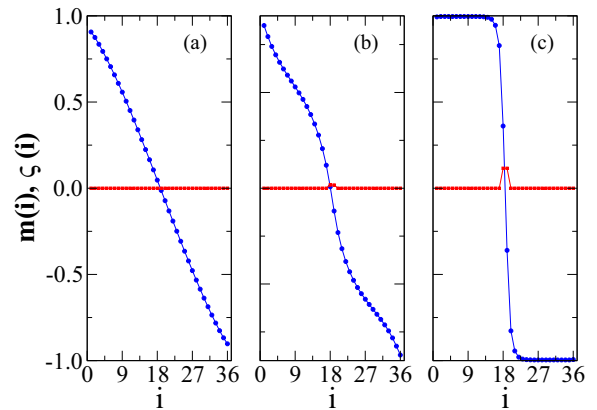


FIG. 3. (Color online) Plots of magnetization profiles $[m(i)]$ versus i and impurity density profiles $[\zeta(i)]$ versus i shown by means of solid circles and squares, respectively. Panels (a) and (b) show data obtained close to second-order wetting transitions, while (c) corresponds to data obtained close to a first-order wetting transition. Measurements performed for (a) $T_w/T_{cb} = 0.73$, $H_{1c}/J = 0.70$, and $D_M = -\infty$, i.e., at the wetting critical point that follows from Abraham's exact solution for the $d = 2$ Ising model [29]. (b) $T/T_{cb} = 0.6875$, $H_1/J = 0.70$, and $D_M/J = -3.0$ and (c) $T/T_{cb} = 0.55$, $H_1/J = 0.70$, and $D_M/J = -0.50$.

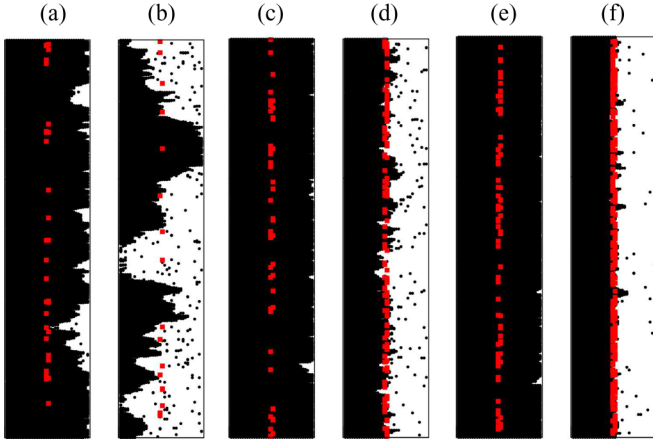


FIG. 4. (Color online) Typical snapshot configurations showing the localization-delocalization transition of the interface for the case of second- and first-order wetting transitions. Data obtained by using samples of size $L = 36$, $M = 1152$, and for $H_1/J = 0.70$. (a) $D_M/J = -3.0$, $T \leq T_w$; (b) $D_M/J = -3.0$, $T \approx T_w$; (c) $D_M/J = -1.75$, $T \leq T_w$; (d) $D_M/J = -1.75$, $T \approx T_w$; (e) $D_M/J = -0.5$, $T \leq T_w$; and (f) $D_M/J = -0.5$, $T \approx T_w$. Spins-up (-down) are shown as circles (left in white), while the impurities are denoted by squares.

critical wetting temperature predicted by the exact solution of Abraham for the Ising model (i.e., $D_M = -\infty$) [29]. In this case, due to the absence of impurities, the observation of a linear profile of the form $m(i) = m_b(1 - 2i/L)$, where m_b is the bulk spontaneous magnetization of the Ising model at $T = T_w$, is observed, as expected from SOS calculations that have already been tested numerically [41]. However, for $D_M/J = -3$ we also have a second-order wetting transition, and such a linear profile becomes largely distorted by the presence of a small amount of impurities but still retains its smooth variation from m_b to $-m_b$. Although the two lines at $i = L/2$ and $i = L/2 + 1$ in the center of the strips where we allow the impurities to be present are a quasi-one-dimensional perturbation of the system only, a dramatic effect on the behavior of the system in the thermodynamic limit $L \rightarrow \infty$ still remains.

The snapshot configurations shown in Figs. 4(a) and 4(b) are also in full qualitative agreement with the above-discussed profiles since they show the localization-delocalization transition of a rather rough interface. This interface performs large excursions in the perpendicular direction of the strips, arriving occasionally at the walls [see Fig. 4(b)]. In contrast to the previously discussed scenario, the profiles measured close to first-order wetting transitions differ substantially [see Fig. 3(c)]. In fact, in this case, on the one hand, one observes a larger density of impurities at the center of the sample and, on the other hand, a distinctively sharp drop of the magnetization from $m_b \approx 1$ to $m_b \approx -1$ that takes place just at the center of the strip. According to this latter observation, a typical set of snapshot configurations shows the dramatic delocalization of the interface that is caused by a small change in temperature [see Figs. 4(e) and 4(f)]. The sharp change observed in the magnetization profile [Fig. 3(c)] is in full agreement with the snapshot shown in Fig. 4(f), where a rather

smooth interface between domains of different orientations is observed at the center of the strip, the vacancies being absorbed along that interface. It is worth mentioning that in our study the interfacial adsorption of impurities is observed only for first-order wetting transitions and is caused by the specific choice of the crystal field [see Eq. (1)], in contrast to the spontaneous interfacial adsorption observed in second-order wetting transitions of the Blume-Capel model [14,15]. The snapshot configurations of Fig. 4(b) with $D_M/J = -3.0$ and Fig. 4(f) with $D_M/J = -0.50$ correspond to well-defined second- and first-order wetting transitions, respectively. On the other hand, Figs. 4(c) and 4(d) with $D_M = -1.75$ show snapshot configurations where the wetting transition is still of first order, but the interface is rougher as compared to the case of Fig. 4(e) but still flatter as compared to the case of Fig. 4(b), qualitatively showing the dependence of the interface width on the strength of the crystal field. Summing up, the analysis of the data shown in Figs. 3 and 4 reveals that a suitable density of nonmagnetic (mobile) impurities randomly distributed along a quasi-one-dimensional defect line can effectively pin the interface between magnetic domains of different orientations.

So, by performing an extensive analysis of our numerical data within the relevant range of parameters (not shown here for the sake of space), we can draw a significant part of the phase diagram that is shown in Fig. 5. Here we used solid-triangle (solid-circle) symbols for second-order (first-order) wetting transitions. The phase diagram shows the existence of lines of second-order transitions that meet first-order lines at tricritical points. Of course, the accuracy of our data is not enough for a precise determination of those tricritical points but suffices to identify the “tricritical neighborhood” that is shown by means of solid-squares in Fig. 5.

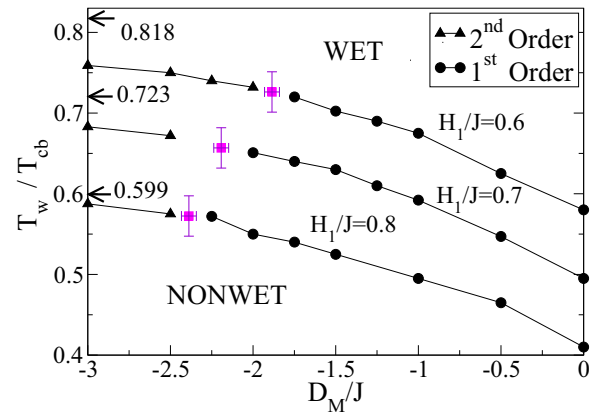


FIG. 5. (Color online) Phase diagram showing the dependence of T_w/T_{cb} versus the crystal field in the center of the strip (D_M) obtained for three different values of the surface magnetic field H_1/J , as indicated. Second- and first-order wetting transitions are denoted by triangles and circles, respectively. The arrows on the left-hand side of the figure show the exact values of T_w/T_{cb} from the analytic results worked out by Abraham [29] and correspond to the Ising model for $D_M = -\infty$. The squares show the estimated location of the tricritical points where first- and second-order curves meet. Curves connecting the points are only drawn to guide the eye. Further details are given in the text.

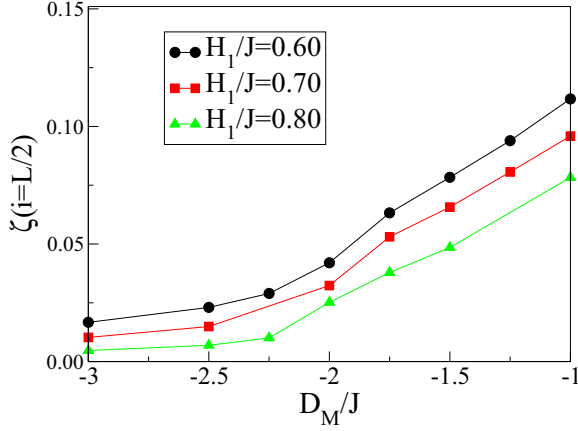


FIG. 6. (Color online) Plots of the densities of nonmagnetic impurities at the center of the sample ($L = 36$, $M = 1152$) as a function of D_M/J . Data obtained at the wetting temperature for different values of H_1/J , as indicated. Curves have been drawn to guide to the eye only.

On the other hand, our choice of the crystal field allows us to compute the density of nonmagnetic impurities at the center of the sample, as shown in Fig. 6. It is found that the curves exhibit monotonically growth without any noticeable deviation close to the tricritical point. Of course, the statistics of our simulations does not allow for a more careful analysis, e.g., in order to evaluate temperature derivatives as in recent work [16].

As already mentioned, it is worth analyzing the dependence of the interface width (w) on D_M within the wet phase for the case of first-order wetting transitions [see Fig. 7(a)]. In fact, it is well known that w can be evaluated just by fitting

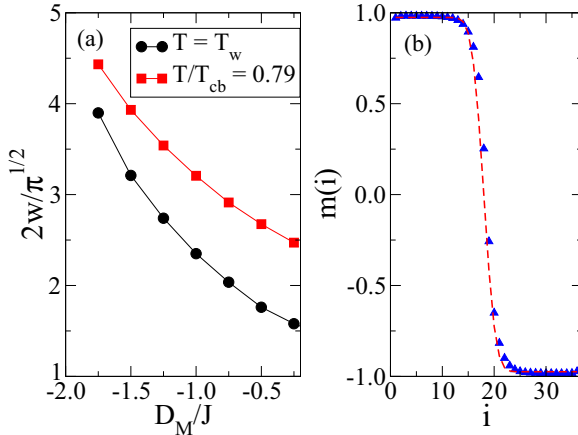


FIG. 7. (Color online) (a) Plots of the interface width (w) versus D_M/J , obtained for samples of size $L = 36$, $M = 1152$, and $H_1/J = 0.60$. Solid circles are obtained along the first-order wetting curve shown in the phase diagram of Fig. 5 for $H_1/J = 0.60$ (upper curve). Solid squares are obtained for $T/T_{cb} = 0.79$, i.e., within the wet phase in the phase diagram of Fig. 5. Panel (b) shows a magnetization profile obtained for a sample of size $L = 36$, $M = 1152$ and $H_1/J = 0.60$, $T_w/T_{cb} = 0.68$, and $D_M = -1.0$. The dashed line corresponds to the best fit of the data performed with the aid of Eq. (9).

magnetization profiles, as shown in Fig. 7(b), with the error function, namely

$$m(i) = m(1)\text{erf}\{\pi^{1/2}(i - L/2)/2w\}. \quad (9)$$

In fact, Fig. 7(b) shows that the sharply varying magnetization profile corresponding to a first-order wetting transition can nicely be fitted with the aid of Eq. (9). So Fig. 7(a) shows that, for both cases, at constant temperature within the wet phase ($T/T_{cb} = 0.79$), as well as for temperatures corresponding to the first-order wetting transitions, the interface width decreases when the density of nonmagnetic species in the center of the sample increases (just by increasing D_M). A somewhat disturbing feature is that the data for w do not indicate the expected vanishing of $1/w$ when D_M approaches the tricritical value; more work on this issue will require much larger systems, unfortunately, and therefore is beyond the scope of the present paper.

IV. THERMODYNAMIC INTEGRATION

In this section, we closely follow our previous presentation in a different context [42]. For interface localization transitions that are strongly first order, the application of finite-size scaling methods (as already discussed in Sec. III [15,17]) offers little advantage [43]. In order to overcome this shortcoming, we conclude that the best way to proceed is to simulate very large systems and locate first-order transitions by equating the free energies of the appropriate phases. These free energies in turn can be accurately obtained by thermodynamic integration [26,27].

Since in the limit of very thick films ($L \rightarrow \infty$), interface localization transitions are predicted to converge toward wetting transitions [44–46], we first discuss how the location of the first-order wetting transitions can be estimated. We note that the free energy of the model [Eqs. (1) and (2)] for large L can be decomposed as [47,48]

$$f(T, H, D, H_1, H_L, L) = f_b(T, H, D) + \frac{1}{L} f_s(T, H, D, H_1) + \frac{1}{L} f_s(T, H, D, H_L). \quad (10)$$

Note that we included the bulk magnetic and crystal fields H and D , respectively. Here $f_b(T, H, D)$ is the free energy (per spin) of a bulk system, which depends on neither H_1 nor H_L . $f_s(T, H, D, H_1)$ is the surface excess free energy of the wall where the field H_1 acts, while $f_s(T, H, D, H_L)$ refers to the surface excess free energy of the wall where H_L acts. As expected, Eq. (10) holds only in the limit of very thick films where the interaction between wetting layers associated with both walls can be neglected. Wetting transitions show up as singularities of the respective surface excess free energies [3,4,7,46,49].

Assuming now $H_1 < 0$, a wetting transition occurs at that surface when $H \rightarrow 0^+$, so we have a positive spontaneous magnetization $m_b(T, H = 0^+, D)$,

$$m_b = -(\partial f_b(T, H, D)/\partial H)_T, \quad (11)$$

in the bulk. In the nonwet phase, $f_s^{(+)}(T, 0, D, H_1)$ then is the excess free energy of a surface where the region of positive

magnetization in the film extends close to the wall where H_1 acts. In the wet phase, however, we have a (macroscopically thick) domain of the negative magnetization adjacent to that wall, separated by an interface (i.e., a domain wall of the same type as that between coexisting oppositely oriented domains in the bulk) from the domain with positive magnetization that takes the bulk of the film. Consequently, the surface excess free energy of a wet surface is

$$f_s^{\text{wet}}(T, 0, D, H_1) = f_s^{(-)}(T, 0, D, H_1) + f_{\text{int}}(T, 0, D). \quad (12)$$

Here $f_s^{(-)}(T, 0, D, H_1)$ is the excess free energy of a surface where both the bulk magnetization and the surface field H_1 are negative, and $f_{\text{int}}(T, 0, D)$ is the interfacial free energy of the model. It is worth mentioning that for the Ising model $f_{\text{int}}(T, 0, -\infty)$, i.e., by taking $D_M = -\infty$ in Eq. (2), this free energy is known exactly since the work of Onsager [28]. However, as we will see below, the presence of two defect lines at $i = L/2$ and $i = L/2 + 1$ in the center of the strips [see Eq. (2)] that represent a quasi-one-dimensional perturbation of the system causes a dramatic effect on the behavior of the system in general and on $f_{\text{int}}(T, 0, D)$ in particular. So the wetting transition occurs when

$$f_s^{(+)}(T, 0, D, H_1) = f_s^{(-)}(T, 0, D, H_1) + f_{\text{int}}(T, 0, D). \quad (13)$$

On the other hand, Eq. (13) can also be derived by using Young's equation for the contact angle Θ , namely

$$f_{\text{int}}(T, 0, D) \cos \Theta = f_s^{(+)}(T, 0, D, H_1) - f_s^{(-)}(T, 0, D, H_1), \quad (14)$$

and taking $\Theta = 0$ [3,4,7,49] at the wetting transition.

In our system, it is convenient to make use of the symmetry relation

$$f_s^{(-)}(T, 0, D, H_1) = f_s^{(+)}(T, 0, D, -H_1), \quad (15)$$

where $f_s^{(+)}(T, 0, D, -H_1)$ is the excess free energy of a surface where the region of positive magnetization in the film extends to a wall where a positive surface field ($-H_1$) acts. Since we are using a film with antisymmetric fields acting at the walls, $H_L = -H_1$, we further conclude that

$$f_s^{(-)}(T, 0, D, -H_1) = f_s^{(+)}(T, 0, D, H_L), \quad (16)$$

and hence the relevant free-energy difference needed to locate the wetting transition simply becomes $\Delta f_{1L} \equiv f_s^{(+)}(T, 0, D, H_1) - f_s^{(+)}(T, 0, D, H_L)$. Using now the relations [47,48]

$$\begin{aligned} m_1 &= -(\partial f_s(T, H, D, H_1) / \partial H_1)_T, \\ m_L &= -(\partial f_s(T, H, D, H_L) / \partial H_L)_T, \end{aligned} \quad (17)$$

we find [note that Eq. (13) of Ref. [42] contains a wrong sign]

$$\begin{aligned} \Delta f_{1L} &= f_s^{(+)}(T, 0, D, H_1) - f_s^{(+)}(T, 0, D, H_L) \\ &= \int_0^{H_1} (m_1^{(-)}(H'_1) + m_L^{(-)}(H'_1)) dH'_1, \end{aligned} \quad (18)$$

by performing a calculation where the surface fields $H'_1 < 0$, $H'_L = -H'_1 > 0$ are varied for a film with positive magnetization. This method for the location of a first-order

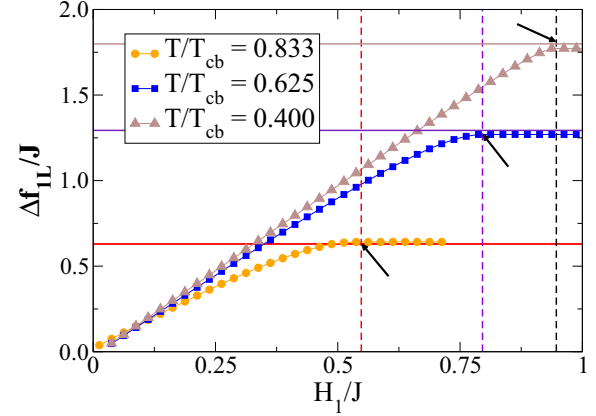


FIG. 8. (Color online) Plots of $\Delta f_{1L}/J$ versus H_1/J obtained at different temperatures (as indicated) and for the case of the Ising model, namely $D_M = -\infty$. Horizontal (solid) lines correspond to the interfacial free energy taken from the exact solution of Onsager [28]. Vertical (dashed) lines correspond to the critical fields of the wetting phase transitions given from the exact solution of Abraham [29]. Intersection points are indicated by means of arrows.

wetting transition has previously been used successfully in the case of symmetric polymer mixtures [50].

In order to evaluate the integral of Eq. (18) in practice, we started at $H_L = -H_1 = 0$ with a system of size $L = 48$ and $M = 2048$, and assumed an ordered initial configuration with all spins pointing up [$S(i, j) = +1$]. Also, we took averages over 3×10^6 MCS, after discarding the first 2×10^6 MCS.

As a test of the accuracy of this procedure, we first applied it to the case $D_M = -\infty$, i.e., the standard problem of wetting in the $d = 2$ Ising model where the answer is known from Abraham's exact solution [29]. Figure 8 plots the results for Δf_{1L} as a function of H_1 obtained for $D_M = -\infty$ (i.e., for the Ising model since vacancies are excluded and no defect line is present). In practice, we found that Eq. (18) can be discretized in steps of $\Delta H_1 = 0.025$ to make the numerical integration error small enough for our purposes (note that fields are quoted in units of J as well). Since for the case of the Ising model ($D_M = -\infty$ in our model) the interfacial free energy is exactly known according to Onsager [28],

$$\sigma = 2J - k_B T \ln \left[1 + \frac{\exp(-2k_B T/J)}{1 - \exp(-2k_B T/J)} \right], \quad (19)$$

in Fig. 8 we included the values of σ corresponding to the temperature where the integration of Eq. (18) was performed (horizontal lines). Additionally, in Fig. 8 we also included the exact results of Abraham [29] for the critical wetting fields (vertical lines), which intercept the integration curves just when they start to become saturated and coincide (within the statistical error) with the lines defining the interfacial free energy. So Fig. 8 shows that by using numerical integration [see Eq. (18)] and taking advantage of the existence of exact results, the location of critical wetting transitions by numerical integration is compatible with the exact results but clearly not an accurate method in practice, since the point where the merging to σ occurs cannot easily be located with high precision.

On the other hand, for values of D_M within our range of interest for the occurrence of first-order wetting transitions (see Fig. 5) one expects that the curve Δf_{1L} will meet σ at a finite nonzero angle. Unfortunately, in the case $D_M > -\infty$ we lack an exact solution for σ , so the interfacial free energy also needs to be found by thermodynamic integration. We thus use here two reference states at very low temperature: (i) a state with all spins pointing up and (ii) a state with the spins adjacent to the wall with $+H_1$ ($-H_1$) pointing up (down), so a flat interface is initially placed along the center of the sample where there is a defect line. The field $H_1 > J$ is fixed so the system magnetization follows the boundary field.

The idea behind the thermodynamic integration method can easily be worked out by using the relationship for the internal energy u per spin

$$u = (\partial(\beta f)/\partial\beta)_{H,D,H_1,H_L}, \quad \beta = 1/T \quad (20)$$

so [26,27]

$$\beta f(\beta) = \beta_0 f(\beta_0) + \int_{\beta_0}^{\beta} u(\beta') d\beta', \quad (21)$$

and one has to record the energy difference between the reference states (which by construction is due to the interface only). Since we are interested in $T < T_{cb}$, using the reference state of infinite temperature ($\beta_0 = 0$) is not convenient, and we would rather use $T = 0$ as a reference state, where the reference free energy $f(\beta_0)$ is trivially known (since the entropy is zero). However, for the thermodynamic integration, Eq. (21), a very large integration interval needs to be avoided, of course, and hence $\beta_0 \rightarrow \infty$ cannot be used. It turns out, however, that $\beta_0 = 20$ is already large enough to neglect the entropy.

Figure 9 shows plots of σ/J versus T/T_{cb} obtained for different values of D_M . For the test case $D_M = -\infty$, we found that the error bars of the numerical integration are smaller than the symbol size. On the other hand, for finite values of D_M the interfacial free energy becomes reduced (at a fixed temperature) as compared to the Ising case due to the presence

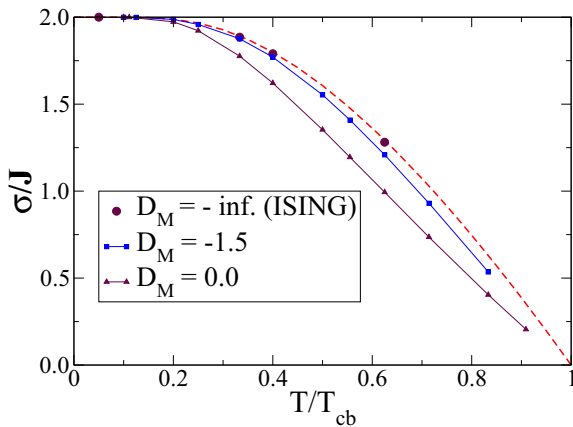


FIG. 9. (Color online) Plots of the interfacial free energy σ/J versus T/T_{cb} obtained at different values of D_M , as indicated. Note that our results for the Ising model (solid circles), namely $D_M = -\infty$, are in agreement with the exact solution of Onsager [see Eq. (19)] shown by a dashed line.

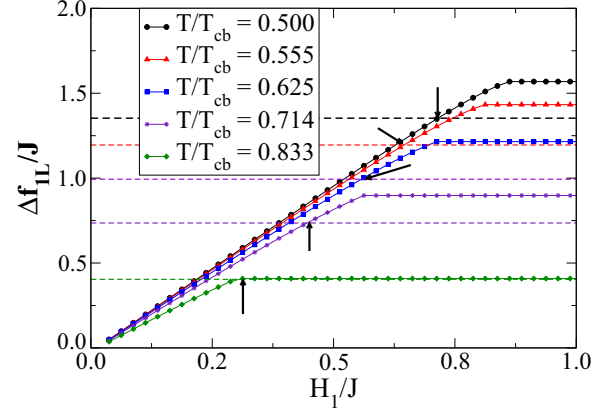


FIG. 10. (Color online) Plots of Δf_{1L} versus H_1/J obtained at different temperatures (as indicated) and for the case $D_M = 0$. Horizontal lines correspond to the interfacial free energy obtained by thermodynamic integration (see Fig. 9). The intersection points at the first-order wetting transitions are shown by means of arrows.

of nonmagnetic impurities at the interface [see Fig. 4(f)], as expected. It is worth mentioning that for the case of a fixed line of vacancies placed equidistantly, as considered in Ref. [20], ground-state considerations yield $f_{FV}^{\text{int}}(T=0)/J = 2(1 - F_v)$, exactly for $F_v \leq 1/2$, where F_v is the fraction of vacancies. Since in the present study the density of vacancies vanish for $T \rightarrow 0$ and the values of the crystal field considered, the interfacial energy is close to the Onsager result [28] $f_{\text{Ons}}^{\text{int}}(T=0)/J = 2$, and therefore differing from (in a factor of the order of $F_v\%$) the case of immobile vacancies. On the other hand, mobile vacancies introduces an additional entropy contribution, e.g., as compared to the case of a line of weakened bonds [30–34], leading to a richer physical behavior, as already discussed in detail in the Introduction.

Focusing now our attention on first-order wetting transitions, Fig. 10 shows plots of the integration results of Δf_{1L} versus H_1 , obtained for $D_M = 0$ and different temperature values. In contrast to the case of critical wetting (see Fig. 8), here we obtained well-defined intersection points that allow us to accurately locate the first-order transition fields (H_{1c}), except for high temperatures (e.g., $T/T_{cb} = 0.833$ in Fig. 10).

Figure 11(a) shows plots of H_{1c}/J versus T/T_{cb} corresponding to first-order wetting transitions. Results obtained by using both the thermodynamic integration method and the location of the abrupt change of the magnetization (see Fig. 2), which are in excellent agreement, are also included in Fig. 11(a). In this way, we can address an additional problem of great interest, namely the first-order wetting behavior near bulk criticality. Note that for a second-order wetting transition one has that

$$H_{1c} \propto (1 - T/T_{cb})^{\Delta_1}, \quad (22)$$

where Δ_1 is a surface critical exponent [51]. The exact solution of Abraham [29] for critical wetting yields $\Delta_1 = 1/2$ in two dimensions. In contrast, our results for first-order wetting transitions in $d = 2$ dimensions seem to be compatible with a linear dependence (i.e., $\Delta_1 = 1$) as follows from a visual inspection of Fig. 11(a) and the test performed in Fig. 11(b). However, we note that deviation from linearity could be

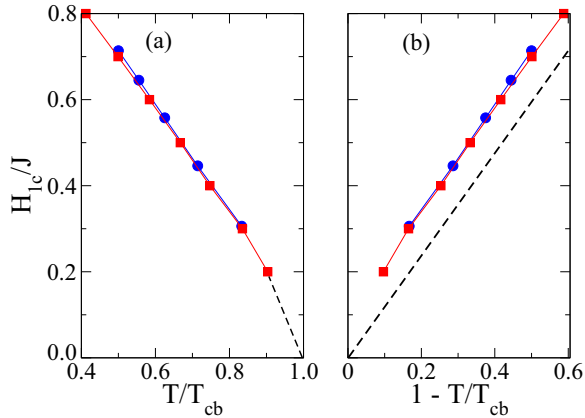


FIG. 11. (Color online) (a) Plots of H_{1c}/J versus T/T_{cb} obtained for the case $D_M = 0$. Results obtained by means of thermodynamic integration are shown in solid circles, while estimations of the location of abrupt drops of the magnetization (see Fig. 2) are shown in solid squares. (b) Plots of H_{1c}/J versus $(1 - T/T_{cb})^{\Delta_1}$, with $\Delta_1 = 1$. The dashed line has been drawn to guide the eye.

expected close to criticality, but a careful study of this topic lies beyond the scope of the present paper.

V. CONCLUSIONS

We studied the wetting behavior of the two-dimensional Ising model confined in a strip with competing boundary fields and a defect line (consisting of two rows adjacent to each other) in the center, where mobile vacancies are allowed to occur (controlled in terms of a suitable crystal field of the Blume-Capel model). Our study on both the influence of a defect line and the role of interfacial adsorption on wetting transitions reveals that by enhancing the density of the inert third phase at

the center of the strip, the nature of the transition changes from second to first order. In this way, tricritical wetting transition points are identified. While interfacial adsorption in the bulk has been studied with the BC model for a long time, in all previous cases the occurrence of only critical wetting has been reported. Our results show that by tuning the density of nonmagnetic impurities adsorbed at the interface, one can change the order of the wetting transition. This result is in qualitative agreement with previous work showing that the same effect is induced by fixed nonmagnetic impurities [20]. The abrupt change in the magnetization profiles from $m_b > 0$ to $m_b < 0$ observed at first-order wetting transitions, where m_b is the spontaneous magnetization at the considered temperature, as well as the flat interfaces characteristically observed in those cases, reveals that suitable nonmagnetic impurities can effectively pin a flat interface. These new features reported in the present paper could be relevant for practical applications aimed at assembling sets of nano- and micromagnetic domains and patterns with sharp interfaces, e.g., for magnetic storage devices. Therefore, we conclude that our paper not only reports issues of theoretical interest, e.g., in the field of statistical mechanics, scaling theory, etc., but also addresses topics of potentially interesting technical applications.

ACKNOWLEDGMENTS

This work was supported by CONICET through PIP 143 and the Universidad Nacional de La Plata, Argentina. One of us (E.V.A.) acknowledges partial support from the Alexander von Humboldt Foundation and from the Schwerpunkt für Rechnergestützte Forschungsmethoden in den Naturwissenschaften (SRFN) to make his visit to the Institut für Physik der Johannes Gutenberg Universität possible. The support of CONICET (Argentina) is also acknowledged. We are grateful to W. Selke for stimulating discussions.

-
- [1] A.-L. Barabási and H. E. Stanley, *Fractal Concepts in Surface Growth* (Cambridge University Press, Cambridge, 1995).
- [2] J. Kertész and T. Vicsek, in *Fractal in Science*, edited by A. Bunde and S. Havlin (Springer-Verlag, Berlin, 1994), p. 89.
- [3] D. E. Sullivan and M. M. Telo da Gama, in *Fluid Interfacial Phenomena*, edited by C. A. Croxton (Wiley, New York, 1986), p. 45.
- [4] S. Dietrich, in *Phase Transitions and Critical Phenomena*, edited by C. Domb and J. L. Lebowitz (Academic, New York, 1988), Vol. XII, p. 1.
- [5] M. Schick, in *Liquids at Interfaces*, edited by J. Charvolin, J.-F. Joanny, and J. Zinn-Justin (Elsevier, Amsterdam, 1990), p. 415.
- [6] G. Forgacs, R. Lipowsky, and T. M. Nieuwenhuizen, in *Phase Transitions and Critical Phenomena*, edited by C. Domb and J. L. Lebowitz (Academic, New York, 1991), Vol. XIV, p. 136.
- [7] D. Bonn and D. Ross, *Rep. Progr. Phys.* **64**, 1085 (2001).
- [8] P. G. De Gennes, F. Brochard-Wyart, and D. Queré, *Capillarity and Wetting Phenomena: Drops, Bubbles, Pearls, Waves* (Springer, Berlin, 2003).
- [9] T. Kissinger, A. Kotowicz, O. Kurz, F. Ginelli, and H. Hinrichsen, *J. Stat. Mech.* (2005) P06002.
- [10] J. Candia and E. V. Albano, *Phys. Rev. Lett.* **88**, 016103 (2001).
- [11] M. R. Moldover and J. W. Cahn, *Science* **207**, 1073 (1980).
- [12] M. Blume, *Phys. Rev.* **141**, 517 (1966).
- [13] H. W. Capel, *Physica* **32**, 966 (1966).
- [14] W. Selke, *Surf. Sci.* **144**, 176 (1984).
- [15] E. V. Albano and K. Binder, *Phys. Rev. E* **85**, 061601 (2012).
- [16] N. G. Fytas and W. Selke, *Eur. Phys. J. B* **86**, 365 (2013).
- [17] E. V. Albano and K. Binder, *Phys. Rev. Lett.* **109**, 036101 (2012).
- [18] A. Pérez-Junquera, V. I. Marconi, A. B. Kolton, L. M. Álvarez-Prado, Y. Souche, A. Alija, M. Vélez, J. V. Anguita, J. M. Alameda, J. I. Martín, and J. M. R. Parrondo, *Phys. Rev. Lett.* **100**, 037203 (2008).
- [19] V. I. Marconi, A. B. Kolton, J. A. Capitán, J. A. Cuesta, A. Pérez-Junquera, M. Vélez, J. I. Martín, and J. M. R. Parrondo, *Phys. Rev. B* **83**, 214403 (2011).
- [20] S. M. Cotes and E. V. Albano, *Phys. Rev. E* **83**, 061105 (2011).
- [21] K. Binder, D. Landau, and M. Müller, *J. Stat. Phys.* **110**, 1514 (2003).
- [22] J. W. Cahn, *J. Chem. Phys.* **66**, 3667 (1977).

- [23] I. Schmidt and K. Binder, *Z. Phys. B* **67**, 369 (1987).
- [24] R. Lipowsky, D. M. Kroll, and R. K. P. Zia, *Phys. Rev. B* **27**, 4499 (1983).
- [25] D. M. Kroll, R. Lipowsky, and R. K. P. Zia, *Phys. Rev. B* **32**, 1862 (1985).
- [26] D. P. Landau and K. Binder, *A Guide to Monte Carlo Simulation in Statistical Physics*, 2nd ed. (Cambridge University Press, Cambridge, 2005).
- [27] K. Binder, *Z. Phys. B* **45**, 61 (1981).
- [28] L. Onsager, *Phys. Rev.* **65**, 117 (1944).
- [29] D. B. Abraham, *Phys. Rev. Lett.* **44**, 1165 (1980).
- [30] D. B. Abraham, *J. Phys. A: Math. Gen.* **14**, L369 (1981).
- [31] S. T. Chui and J. D. Weeks, *Phys. Rev. B* **23**, 2438 (1981).
- [32] T. W. Burkhardt, *J. Phys. A* **14**, L63 (1981).
- [33] J. M. J. van Leeuwen and H. J. Hilhorst, *Physica A* **107**, 319 (1981).
- [34] D. Todorović and N. M. Švrakić, *Z. Phys. B. (Condens. Matter)* **87**, 355 (1992).
- [35] W. Selke, N. M. Švrakić, and P. J. Upton, *Z. Phys. B. (Condens. Matter)* **89**, 231 (1992).
- [36] M. E. Fisher, *J. Stat. Phys.* **34**, 667 (1984).
- [37] T. W. Burkhardt and E. Eisenriegler, *Phys. Rev. B* **24**, 1236 (1981).
- [38] S. Sarbach and I. D. Lawrie, in *Phase Transitions and Critical Phenomena*, edited by C. Domb and J. L. Lebowitz, Vol. 9 (Academic, London, 1984), p. 1.
- [39] R. da Silva, N. A. Alves, and J. R. Drugowich de Felício, *Phys. Rev. E* **66**, 026130 (2002).
- [40] K. Binder, *Rep. Prog. Phys.* **60**, 487 (1997).
- [41] E. V. Albano, K. Binder, and W. Paul, *J. Phys.: Condens. Matter* **12**, 2701 (2000).
- [42] E. V. Albano and K. Binder, *J. Stat. Phys.* **135**, 991 (2009).
- [43] A. M. Ferrenberg, D. P. Landau, and K. Binder, *Phys. Rev. E* **58**, 3353 (1998).
- [44] A. O. Parry and R. Evans, *Physica A* **181**, 250 (1992).
- [45] A. O. Parry and R. Evans, *Phys. Rev. Lett.* **64**, 439 (1990).
- [46] K. Binder, D. P. Landau, and M. Müller, *J. Stat. Phys.* **110**, 1411 (2003).
- [47] K. Binder and P. C. Hohenberg, *Phys. Rev. B* **6**, 3461 (1972); **9**, 2194 (1974).
- [48] K. Binder, in *Phase Transitions and Critical Phenomena*, edited by C. Domb and J. L. Lebowitz (Academic Press, New York, 1983), Vol. 8, p. 1.
- [49] P. G. de Gennes, *Rev. Mod. Phys.* **57**, 827 (1985).
- [50] M. Müller and K. Binder, *Macromolecules* **31**, 8323 (1998).
- [51] H. W. Diehl, *Int. J. Mod. Phys. B* **11**, 3503 (1997).